

Elastic modulus of PVDF with bentonite or LiNbO₃ using deformation energy

Carlos Alberto Fonzar Pintão^{1*} and Celso Xavier Cardoso²

¹*Department of Physics, Faculty of Science, Universidade Estadual Paulista “Julio de Mesquita Filho” – UNESP, Bauru, SP, Brazil*

²*Department of Physics, Chemistry and Biology, Faculty of Science and Technology, Universidade Estadual Paulista “Julio de Mesquita Filho” – UNESP, Presidente Prudente, SP, Brazil*

*fonzar@fc.unesp.br

Abstract

Polyvinylidene fluoride (PVDF) is valued for its properties of transparency to light, lightness, flexibility, mechanical strength, chemical stability, ease of processing, and low-cost production. Ceramics have low mechanical strength and poor processability, but have excellent piezo- and pyroelectric characteristics. The deficiencies of ceramics can be minimized by combining them with polymers. Accordingly, PVDF samples with different percentages of bentonite or LiNbO₃ were used to obtain composites via “casting,” and the modulus of elasticity (E) of the composites was studied using a specially designed system. The method used to obtain E took into account the strain energy and the strength of the materials. Based on the results, E decreased with an increased percentage of bentonite and, in the case of LiNbO₃, for the percentages of 30% and 35% increases.

Keywords: *bentonite, deformation energy, LiNbO₃, modulus of elasticity, PVDF.*

1. Introduction

This study uses a specially designed system to determine the modulus of elasticity (E) of the tensile strength of polymer composites. Several methods and techniques can be used to obtain E, including static testing (tensile, torsion, bending), dynamic testing (resonant frequency method), wave propagation methods (ultrasonic echo-pulse method), and nanoindentation testing. Each method has advantages and disadvantages. Moreover, the measured Young’s modulus values obtained from these methods are different, even for the same sample material. Of these methods, the pulse-echo ultrasound method is most commonly used^[1,2]. This technique is nondestructive and does not alter the sample’s physical or chemical properties; thus, it has significant practical interest. However, the pulse-echo ultrasound method can only measure E values for a single sample temperature and for well-defined sizes. In such cases, Poisson coefficient information is needed to obtain E, and the sample dimensions may be crucial. Clay and polymeric materials have complementary characteristics regarding the preparation of ferroelectric materials. Such materials are widely used in the electronics, sensors, and transducers industries, which require piezoelectric materials and easy processability. We used polyvinylidene fluoride (PVDF), which is an important transducer material because of its mechanical resistance, chemical inertness^[3], and high piezoelectricity^[4]. PVDF is used in hydrophones, industrial acoustic materials, and vibration sensors. Depending on the conditions used to process PVDF, it presents at least four crystalline phases, known as α , β , γ , and δ ^[5-7]. PVDF has a spherulitic crystallization morphology in which the spherulites are formed by lamellar crystalline regions, which grow from the center to the edges in a radial direction, and by amorphous regions, located between the crystalline lamellae

of the spherulites^[8,9]. In a dimethylformamide (DMF) solution from which, in the crystallization of PVDF, both the α and β phases are obtained, it has been found^[10] that, depending on the crystallization temperature (T), the predominantly α -phase films crystallize at $T < 160$ °C. The influence of the PVDF phases is scientifically and technologically important because these phases can influence the physical and chemical properties of PVDF. In addition, PVDF is easy to process and its production costs are low^[11]. Unfortunately, neat PVDF cannot completely meet the mechanical, thermal, and oxidation resistance property requirements of some harsh environments^[12,13]. Many efforts have been made to improve the properties of PVDF. For example, the incorporation of organic polymers or inorganic fillers into the PVDF matrix to produce composites has been extensively studied to further improve its properties^[14,15]. This present study aims to introduce and apply a technique to measure the modulus of elasticity (E) of polymeric composites.

2. Materials and Methods

The casting method was used to incorporate ceramic LiNbO₃ or bentonite into the PVDF, in which the PVDF grains (Florafon F4000 HD; Atochem) were dissolved in DMF under stirring and heating at 100 °C for 30 minutes in a shaker magnetic heater. The ceramics were dispersed in the DMF, and they were mixed with and dissolved in the PVDF. After stirring and heating the mixture for 10 minutes until it was homogenized, the resulting solution was poured into petri dishes and placed in an oven at 100 °C for three hours to dry and evaporate the solvent. Once all the samples were prepared, they were cut and fixed, one at a time, and

measurements were taken (Figure 1A). A caliper or micrometer was used to obtain the parameters (a and b) for determining the area of the rectangular cross-section (A) and the length (L) at the instant the tensile force was applied (Figure 1B). The values for six samples of PVDF/LiNbO₃, with increasing percentages, by weight, of LiNbO₃, are shown in Table 1, while the values for 10 samples of PVDF/bentonite, with increasing percentages, by weight, of the bentonite, are presented in Table 2.

2.1 Deflection energy method for obtaining E

Consider an elastic structure submitted to applied loads and deformed elastically. In this deformation process, the principle of energy conservation^[16] is used, expressed as:

$$W_E + Q = \Delta E \quad (1)$$

W_E is the work carried out by the applied external forces, Q is the heat that the structure exchanges with its surrounding area, and ΔE is the variation in the associated energies of the structure: kinetic energy (K) and internal energy (U). Considering that the increase in these loads is gradual and that a state of equilibrium is maintained during this process, then the variation of kinetic energy is zero and ΔE is due only to the variation in internal energy U. Under these conditions, Equation 1 is reduced to:

$$W_E = \Delta U \quad (2)$$

The work, which is energy stored in the structure due to tensile force in an infinitesimal volume element^[6,7], is represented by the strain and stress tensors, σ_{ij} and ϵ_{ij} , respectively. The energy, dU, which is stored in this element when the deformation has reached its final value ϵ_{ij} , is:

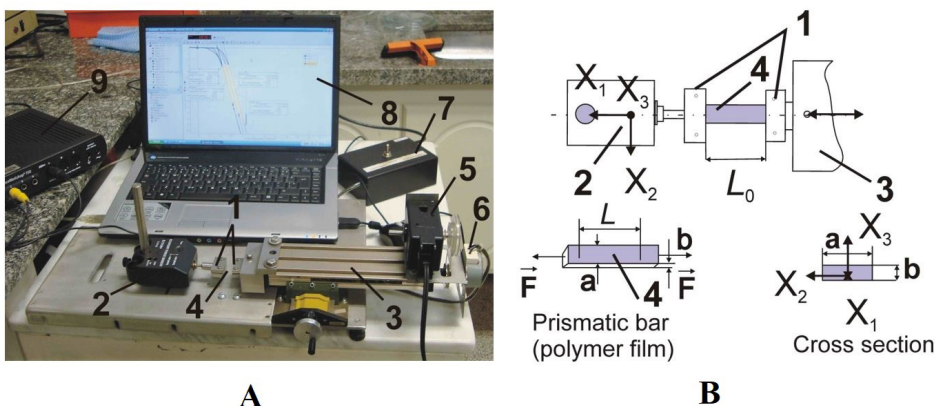


Figure 1. (A) System for measuring E: (1) Pieces of attachment of samples; (2) Force sensor (FS-PASCO: CI6537); (3) XY table; (4) Samples: PVDF/LiNbO₃ or PVDF/Bentonite; (5) Rotational movement sensor (RMS-PASCO: CI6538; [8]); (6) Motor for moving XY table; (7) Key to activate motor; (8) Computer with specific software; (9) Interface (PASCO: CI7650-750); (B) Schematic diagram of the XY table, Pieces of attachment of samples and FS; Cross section of sample of area A; Prismatic bar width a, height b and length L.

Table 1. Results of PVDF/LiNbO₃.

LiNbO ₃ , wt. %	B ₀ (N/rad)	L (mm)	a (mm)	b (mm)	A (mm ²)	E (MPa)
4	1.480 ± 0.004	18.23 ± 0.05	15.45 ± 0.05	0.04 ± 0.01	0.6 ± 0.1	1510 ± 378
10	1.347 ± 0.004	13.66 ± 0.05	15.50 ± 0.05	0.03 ± 0.01	0.5 ± 0.2	1369 ± 458
15	0.727 ± 0.002	12.67 ± 0.05	13.75 ± 0.05	0.04 ± 0.01	0.6 ± 0.1	579 ± 145
25	0.727 ± 0.002	12.67 ± 0.05	13.75 ± 0.05	0.04 ± 0.01	0.6 ± 0.1	579 ± 145
30	7.34 ± 0.02	8.48 ± 0.05	11.6 ± 0.05	0.07 ± 0.01	0.8 ± 0.1	2651 ± 379
35	4.97 ± 0.02	5.29 ± 0.05	10.7 ± 0.05	0.04 ± 0.01	0.4 ± 0.1	2126 ± 532

Table 2. Results of PVDF/bentonite.

bentonite, wt. %	B ₀ (N/rad)	L (mm)	a (mm)	b (mm)	A (mm ²)	E (MPa)
1	5.45 ± 0.01	12.26 ± 0.05	8.80 ± 0.05	0.15 ± 0.01	1.32 ± 0.09	1752 ± 118
3	5.62 ± 0.02	12.38 ± 0.05	10.50 ± 0.05	0.16 ± 0.01	1.7 ± 0.1	1435 ± 91
4	7.05 ± 0.02	11.96 ± 0.05	12.05 ± 0.05	0.15 ± 0.01	1.8 ± 0.1	1613 ± 108
5	6.52 ± 0.01	10.89 ± 0.05	9.20 ± 0.05	0.21 ± 0.01	1.93 ± 0.09	1271 ± 61
10	6.59 ± 0.02	11.37 ± 0.05	12.20 ± 0.05	0.14 ± 0.01	1.71 ± 0.01	1518 ± 109
15	6.52 ± 0.01	11.37 ± 0.05	11.60 ± 0.05	0.18 ± 0.01	2.09 ± 0.01	1228 ± 69
20	7.26 ± 0.02	10.28 ± 0.05	12.20 ± 0.05	0.20 ± 0.01	2.4 ± 0.1	1057 ± 53
25	5.93 ± 0.02	10.11 ± 0.05	12.80 ± 0.05	0.22 ± 0.01	2.8 ± 0.1	737 ± 34
30	6.63 ± 0.04	10.66 ± 0.05	13.90 ± 0.05	0.20 ± 0.01	2.8 ± 0.1	880 ± 45
35	2.90 ± 0.01	13.40 ± 0.05	13.30 ± 0.05	0.23 ± 0.01	3.06 ± 0.01	439 ± 19

$$dU = \int_0^{e_{ij}} \sigma_{ij} de_{ij} \quad (3)$$

By integrating the total volume (V) of the structure, we obtain the total internal energy U due to the deflection, which is expressed as:

$$U = \int_0^{e_{ij}} \left(\int_0^V \sigma_{ij} de_{ij} \right) dV \quad (4)$$

In cases where the elastic structure shows linear behavior, it is isotropic, and it is subjected to pure tensile stress. Using Hooke's law^[16], it is established that:

$$U = \int \frac{1}{2E} \sigma_{11}^2 dV \quad (5)$$

where E is the modulus of elasticity of the tensile force.

To measure E, a prismatic bar is used with a uniform cross-section of area A and length L, subjected to applied force F by a force sensor (FS) at one end with another attached to XY table (Figure 1A and B).

With regard to material resistance^[17], it is known that the stress state of an internal point of a polymer, x_i , based on the experimental conditions shown in Figure 1, is expressed as:

$$\sigma_{11} = \frac{F}{A} \quad (6)$$

The cross-sectional area is represented by A, which is given by the product of the sides: width (a) and height (b). Substituting this stress component in Equation 5 yields the internal strain energy in the structure for this specific application:

$$U = \frac{F^2 L}{2EA} \quad (7)$$

The external work conducted by F is:

$$W_E = F \Delta L \quad (8)$$

From Equation 7 and Equation 8, we obtain:

$$F = \frac{2EA}{L} \Delta L = B^* \Delta L \quad (9)$$

If we replace the values of the cross-sectional area (A) and use B* and the calibration factor of the force sensor (f), we obtain the equation for the calculation of E:

$$E = \frac{B^* L}{2A} f \quad (10)$$

2.2 Measurement of the modulus of elasticity of tensile force

A rotation movement sensor (RMS) was used to measure the turning angle, φ (rad), of the screw that moves the XY table when it shifts from ΔL ^[18]. A pulley, with a diameter of $\phi=28.70 \pm 0.05$ mm, was attached to the RMS shaft. With the belt that passes through this pulley, and in the other pulley of the same diameter ϕ affixed to the shaft of the table

transmission mechanism, one can register φ . On the same side as the rotation sensor, we used a microwave motor with a constant torque to move the XY table in the two required directions: one for approximation and the other for drawing XY table away from the force sensor. One piece of the XY table is attached to the opposite side of the rotation sensors, and screws are used to fix one side of the sample. The force sensor (FS) has a fixture that is similar to that of the table. That fixture is attached with a screw to the other end of the sample (Figure 1A and B). The FS is fixed to a steel base that sits on a countertop. Turning the screw moves the XY table at an angle φ (rad), displacing the sample. The motion is measured by ΔL , i.e., φ (0.000160 m).

Thus, tensile force is slowly applied to the sample by force F. FS is zeroed before measuring F. The value of F is automatically recorded for each angle φ with an RMS. The two sensors are connected at an interface to a computer. Using PASCO software, the experimental points for F (N) and φ (rad) are obtained in real-time, simultaneously. Thus, we can adjust the straight line and obtain the slope of B_0 because the points are linear in a regime in which the material shows elastic behavior. The slope B_0 has units expressed in N/rad, which is transformed to N/m using the $B^*=B_0$ (1/0.000160) ratio, since it was evaluated for the measurement system in question where 1 rad equals 0.000160 m.

To determine these measurements, we had to obtain a calibration factor (f) because the value of F measured (F_{MEASURED}) in FS is different from that of F applied (F_{APPLIED}). Factor f can be obtained experimentally by applying known forces (F_{APPLIED}), and then measuring the forces with FS (F_{MEASURED}). For this, we used known masses: 0.020 kg, 0.050 kg, 0.100 kg, 0.200 kg, 0.500 kg, and 1.00 kg. They were fixed at one end of an inextensible cord passing over a pulley at the other end, and attached to FS. Before placing the samples of polymer/LiNbO₃ or polymer/bentonite into clamps, their dimensions (a and b) were measured with a caliper and a micrometer.

At the beginning of the experiment, the samples were fixed on the XY table and FS by locking the components without an applied tensile force. L_0 was measured with a caliper. The length, L, was obtained from the curve of force F (N) as a function of the angle φ (rad). For each of the samples studied, three measures of F as a function of the angle φ were obtained. The first measurement was very important for providing information about how many rotations (φ [rad]) were needed to turn the screw of the XY table to exert tensile force on the sample. L is reported as the sum of ($L_0 + \varphi$ [0.00016 m]). For the second and third measures, the screw was turned counterclockwise to apply new tensile force again, taking care to drive the XY table into a position where the sample would not be submitted to initial tensile stress. The value of L, which was the same as that measured in the first experimental curve (F as a function of φ), was used in Equation 10. At the beginning of every measurement, the force sensor was reset.

3. Results and Discussion

The results presented in Figure 2 show the calibration curve of the FS. The value obtained was $f = 11.0697 \pm 0.0003$. This value was used in Equation 10 to obtain E. A typical curve, F , as a function of ϕ for a PVDF/LiNbO₃ (65/35 wt. %) composites, is shown in Figure 3. The slope B_0 of the three curves shown in Figure 3 was obtained by fitting a straight line to each of the curves when they showed the linear behavior that is characteristic of an elastic regime. For the proposed method to be applied, it is important that a region on the curve of force F (N) as a function of the angle ϕ (rad) represents linear behavior. In our experimental procedure, the limits of elasticity of these samples were not exceeded. Thus, we achieved good reproducibility for the E value. On the other hand, a different procedure can be adopted that uses various samples cut from the same sample source. Then, the complete experimental curve (F as a function of ϕ) can be determined for each sample. In that case, we can determine E using the strain energy method. It is possible to obtain the values of the forces for the limit of elasticity and for the rupture of the sample. Toward that end, we must consider the maximum load limits of FS (± 20 N). Because we had a number of reduced samples, we chose the method described in this paper. An examination of the samples under a microscope shows the presence of isotropic and anisotropic structures, which could be due to the method in which these compounds were prepared^[5]. This may explain the greater or lesser rigidity of the samples when adding increasing mass percentages of LiNbO₃. The procedure to obtain E shows that these samples behaved as an elastic structure, but that does not mean that they were completely isotropic, and it does not invalidate the proposed method. As the crystallization temperature is decreased to < 160 °C, it is expected that there would be a predominance of the α phase^[8-10]. For each PVDF sample with different percentages of LiNbO₃, we calculated the average value of B_0 , measured by the sensors FS and RMS, relative to the three measurements of the curves as a function of the angular position. Equation 10 was then used to calculate the value of E. The results are shown in Table 1.

Figure 4 shows the final results of E, which is expressed in MPa for all the studied samples with increasing percentages of LiNbO₃. Using our method, the E value of the PVDF was close to 2000 MPa, which is close to the expected value^[19].

A typical curve, F , as a function of ϕ for a composite based on PVDF/bentonite (90/10 wt. %), is shown in Figure 5. The same procedure for PVDF/LiNbO₃ was performed for PVDF/bentonite. For each PVDF sample with different percentages of bentonite, we calculated the average value of B_0 , measured by the sensors FS and RMS, relative to the three measurements of the curves as a function of the angular position. Equation 10 was then used to calculate the value of E. The results are shown in Table 2.

Figure 6 shows the final results of E, which is expressed in MPa for all the studied samples with increasing percentages of bentonite. In this case, the rigidity of the composite decreases with the increasing percentage, by weight, of bentonite.

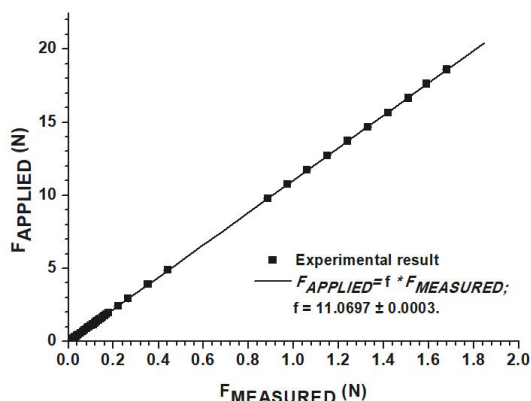


Figure 2. Calibration curve of the force sensor. The calibration factor f is 11.0697 ± 0.0003 .

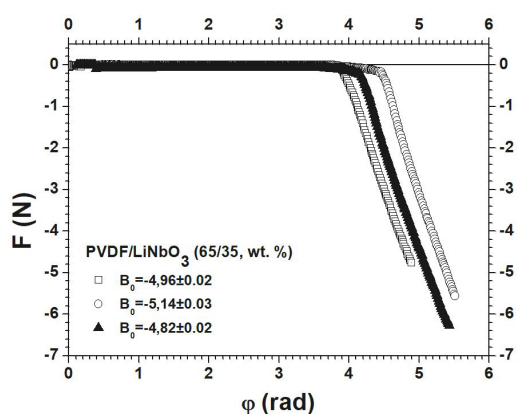


Figure 3. Typical curves of force F (N) as a function of the angular position ϕ (rad). Sample of PVDF/LiNbO₃; $L_0 = 4.65 \pm 0.05$ mm; $L = 4.65 + 4.0(0.16) = 5.29$ mm ± 0.05 mm; $a = 10.70 \pm 0.05$ mm; $b = 0.04 \pm 0.01$ mm; $A = 0.4 \pm 0.1$ mm²; $B_0 = 4.97 \pm 0.02$ N/rad; $B^* = 31083 \pm 148$ N/m. E is calculated using Equation 10: $E = 2126 \pm 532$ MPa.

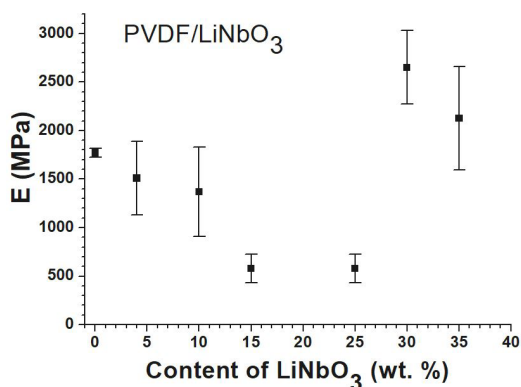


Figure 4. Experimental values of E obtained in the samples (PVDF/LiNbO₃) at different percentages by weight. The value of E for the sample PVDF/LiNbO₃ (100/0, wt. %) was obtained according to Wallner et al.^[19], that is, 1771 ± 46 MPa.

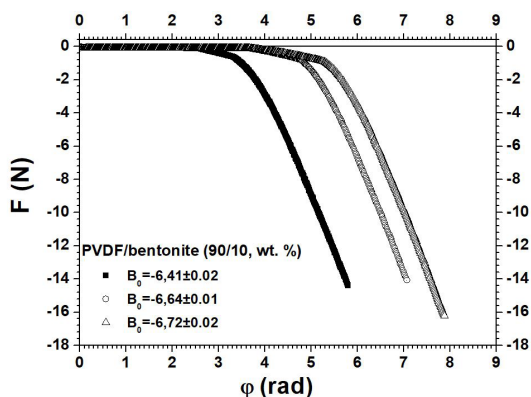


Figure 5. Typical curves of force F (N) as a function of the angular position ϕ (rad). Sample of PVDF with bentonite: $L_0 = 11.00 \pm 0.05$ mm; $L = 11.00 + 2.3(0.16) = 11.37$ mm ± 0.05 mm; $a = 12.20 \pm 0.05$ mm; $b = 0.14 \pm 0.01$ mm; $A = 1.71 \pm 0.01$ mm²; $B_0 = 6.59 \pm 0.02$ N/rad; $B^* = 41188 \pm 119$ N/m. E is calculated by Equation 10: $E = 1518 \pm 109$ MPa.

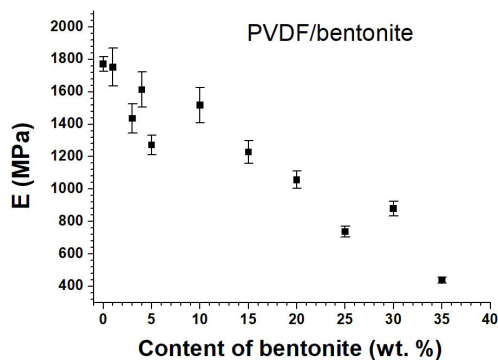


Figure 6. Experimental values of E obtained from the samples (PVDF/bentonite) at different percentages by weight. The value of E for the sample PVDF/bentonite (100/0, wt. %) was obtained according to Wallner et al.^[19], that is, 1771 ± 46 MPa.

4. Conclusions

The system described in this study is an alternative method for obtaining E in polymer composites. This method took into account the tensile strain energy and the strength of the materials. The method was applied to PVDF samples with different percentages, by weight, of LiNbO_3 or bentonite. It can be used with other types of materials in cases where the elastic structure shows linear behavior. Based on our results, the studied samples showed variations in the values of E when the percentage of LiNbO_3 or bentonite changed. The values of E decreased as the percentage of bentonite increased. The value of E increased when the percentages, by weight, for LiNbO_3 were 30% and 35%.

5. Acknowledgements

The authors thank FAPESP, process number: 2007/04094-9, and CAPES, process number: BEX 6571/14-0.

6. References

1. Truel, R., Elbaum, C., & Chic, B. B. (1969). *Ultrasonic methods in solid state physics*. New York: Academic Press.
2. Nowick, A. S., & Berry, B. S. (1972). *Anelastic relaxation in crystalline solids*. New York: Academic Press.
3. Roh, Y., Varadan, V. V., & Varadan, V. K. (2002). Characterization of all the elastic, dielectric, and piezoelectric constants of uniaxially oriented poled PVDF films. *IEEE Transactions on Ultrasonics, Ferroelectrics, and Frequency Control*, 49(6), 836-847. PMID:12075977. <http://dx.doi.org/10.1109/TUFFC.2002.1009344>.
4. Motyl, E. (2001). Comparison between step and pulsed electroacoustic techniques using both PVDF and LiNbO_3 transducers. *Journal of Electrostatics*, 51-52, 530-537. [http://dx.doi.org/10.1016/S0304-3886\(01\)00064-X](http://dx.doi.org/10.1016/S0304-3886(01)00064-X).
5. Costa, C. M., Mendes, S. F., Sencadas, V., Ferreira, A., Gregorio, R. Jr, Ribelles, J. L. G., & Méndez, S. L. (2010). Influence of processing parameters on the polymer phase, microstructure and macroscopic properties of poly (vinilidene fluoride)/ $\text{Pb}(\text{Zr}_{0.53}\text{Ti}_{0.47})\text{O}_3$ composites. *Journal of Non-Crystalline Solids*, 356(41-42), 2127-2133. <http://dx.doi.org/10.1016/j.jnoncrysol.2010.07.037>.
6. Mendes, S. F., Costa, C. M., Caparros, C. V., Sencadas, V. S., & Lanceros-Méndez, S. (2012). Effect of filler size and concentration on the structure and properties of poly(vinylidene fluoride)/ BaTiO_3 nanocomposites. *Journal of Materials Science*, 47(3), 1378-1388. <http://dx.doi.org/10.1007/s10853-011-5916-7>.
7. Mendes, S. F., Costa, C. M., Sencadas, V., Nunes, J. S., Costa, P., Gregorio, R., Jr., & Méndez, S. L. (2009). Effect of the ceramic grain size and concentration on the dynamical mechanical and dielectric behavior of poly (vinilidene fluoride)/ $\text{Pb}(\text{Zr}_{0.53}\text{Ti}_{0.47})\text{O}_3$ composites. *Applied Physics A: Materials Science & Processing*, 96(4), 899-908. <http://dx.doi.org/10.1007/s00339-009-5141-2>.
8. Lovinger, A. J. (1982). Developments in crystalline polymers. *Journal of Polymer Science Part C: Polymer Letters*, 20(10), 559-560. <http://dx.doi.org/10.1002/pol.1982.130201011>.
9. Broadhurst, M. G., Davis, G. T., Mckinney, J. E., & Collins, R. E. (1978). Piezoelectricity and pyroelectricity in polyvinylidene fluoride: a model. *Journal of Applied Physics*, 49(10), 4992-4997. <http://dx.doi.org/10.1063/1.324445>.
10. Gregorio, R., Jr., & Cestari, M. (1994). Effect of crystallization temperature on the crystalline phase content and morphology of poly(vinylidene fluoride). *Journal of Polymer Science. Part B, Polymer Physics*, 32(5), 859-870. <http://dx.doi.org/10.1002/polb.1994.090320509>.
11. Inderherbergh, J. (1990). Polyvinylidene fluoride (PVDF) appearance, general properties and processing. *Ferroelectrics*, 115(4), 295-302. <http://dx.doi.org/10.1080/00150193.1991.11876614>.
12. Dargaville, T. R., Celina, M., & Chaplya, P. M. (2005). Evaluation of piezoelectric Poly (vinylidene fluoride) polymers for use in space environments. I. Temperature limitations. *Journal of Polymer Science. Part B, Polymer Physics*, 43(11), 1310-1320. <http://dx.doi.org/10.1002/polb.20436>.
13. Dargaville, T. R., Celina, M., Martin, J. W., & Banks, B. A. (2005). Evaluation of piezoelectric PVDF polymers for use in space environments. II. Effects of atomic oxygen and vacuum UV exposure. *Journal of Polymer Science. Part B, Polymer Physics*, 43(18), 2503-2513. <http://dx.doi.org/10.1002/polb.20549>.
14. Malmonge, L. F., Langiano, S. C., Cordeiro, J. M. M., Mattoso, L. H. C., & Malmonge, J. A. (2010). Thermal and Mechanical Properties of PVDF/PANI Blends. *Materials Research*, 13(4), 465-470. <http://dx.doi.org/10.1590/S1516-14392010000400007>.

15. Xu, H. P., Dang, Z. M., Jiang, M. J., Yao, S. H., & Bai, J. (2008). Enhanced dielectric properties and positive temperature coefficient effect in the binary polymer composites with surface modified carbon black. *Journal of Materials Chemistry*, 18(2), 229-234. <http://dx.doi.org/10.1039/B713857A>.
16. Tauchert, T. R. (1974). *Energy principles in structural mechanics*. New York: McGraw-Hill.
17. Timoshenko, S. P., & Goodier, J. N. (1980). *Theory of elasticity*. 3rd ed. Rio de Janeiro: Guanabara Dois.
18. Pasco Scientific. (1996). *User's Guide: Science Workshop™ Interface, Version 2.2*. Roseville: Pasco Partners LLC.
19. Wallner, G. M., Major, Z., Maier, G. A., & Lang, R. W. (2008). Fracture analysis of annealed PVDF films. *Polymer Testing*, 27(3), 392-402. <http://dx.doi.org/10.1016/j.polymertesting.2008.01.006>.

Received: May 31, 2016

Revised: Oct. 20, 2016

Accepted: Nov. 10, 2016